Proceedings of The Korea-Russia Joint Conference on
Advanced Sciences and Technologies. *June, 1998, Korea*

Optimized PWM Switching Strategy for an Induction Motor Voltage Control

Hae-Kyung Lee*, Seuk-Yung Hwang**

* Department of Electronic Engineering, KyungWon College, Songnam Korea
** Department of Electric Engineering, DanKuk Univ., Seoul Kore

Abstract

An optimized PWM switching strategy for an induction motor voltage control is developed and demonstrated. Space vector modulation in voltage source inverter offers improved DC-bus utilization and reduced commutation losses, and has been therefor recognizedas the prefered PWM method, especially in the case of digital implementation.

Three-phase invertor voltage control by space vector modulation consists of switching between the two active and one zero voltage vector by using the proposed optimal PWM algorithm.

The prefered switching sequence is defined as a fonction of the modulation index and period of a carrier wave. The suquence is selected by suing the inverter switching losses and tne current ripple as the criteria.

For low and medium power application, the experimental results indicate that good dynamic response and reduced harmonic distortion can be achived by increasing switching frequency.

I. Introduction

The purpose of PWM is to generate an output waveform with desired frequency and magnitudes with a composition pulses of variable width from a given constant magnitude input. Even thought the output voltage waveform of idea inverters should be sinusodial, the waveform of practical inverters is non-sinusodial and contain harmonics [1].

The desirability of a given method depends on :

- harmonic distortion of the output waveform for a given switching frequency
- utilization of a DC bus voltage
- dynamic response
- ease of implementation

The most preferred PWM technique today is space vector modulation[2],[3],[4] which offers 15% better bus utilization and 33% fewer commutations per cycle than conventional PWM.

Since the space vector modulation offerssuperior rerformance with respect to other modulation technique, both establishing the sequencing strategy on microprocessor -implemented PWM control scheme which is the best suitable for variable frequency AC drives and developing and efficient and simple strategy to obtain the desired performance criteria are equally important.

The analytical expression is drived for the RMS value of the current ripple as a function of the modulation index. Experimental data comsist of the stator current waveforms and its line voltage spectra of and induction motor.

In the proposed scheme, the switching patterns are directly generated by means of on-line computations and stored by look-up table memory. The system memory requirement and CPU time are reduced because the scheme only needs the precalculation of a mimimum number of switching points per half cycle. The witching strategies are determined by varying the

II. Space vector modulation

The space vector modulation and problem of selecting the appropriate switching sequence are clearly understood if the phase quantities are transformed into the $\alpha-\beta$ stationary reference frame :

$$U_\alpha = U_a - \frac{U_b + U_c}{2},$$

$$U_\beta = \frac{\sqrt{3}}{2} \times (U_b - U_c) \quad (1)$$

Assuming that the reference U is in sector 1, at Fig.1 and that it has an amplitude A and the angle θ = arg (U) with respect to the α axes. The time intervals T_1, T_2 and T_0 are given by :

$$T_1 = T \cdot m \cdot \sin(60^\circ - \Delta\theta) \quad (2)$$

$$T_2 = T \cdot m \cdot \sin(\Delta\theta) \quad (3)$$

$$T_0 = T - T_1 - T_2 \quad (4)$$

where, A : woltage vector amplitude,
m = A/d : modulation index,
d = E · sin(60 °) : Tne diameter of an inscribed circle in the hexagon,
$\Delta\theta$ = arg (U) - arg (V_1) : The displacement between hte reference U and the clockwise-side V_1 vector .

The voltage vector is applied as following rules : the voltage vector V_1 is applied during the interval T_1 and the vector V_2 is applied during the interval T_2 and the zero vector is applied during the interval T_0. The equationse (2)-(4) defines the intervals T_n, T_{n+1} and T_0 for any other sector in the hexagon. Depending on the spatial orientation of the voltage reference U, each modulation cycle should consist of the sequence of vectors V_n, V_{n+1} and $V_{7/8}$, where $n \in [1, 2, \cdots, 6]$ is the sector number, while the angle

$\Delta\theta = \arg(U) - (n-1) \times 60^\circ$.

The zero vector is applied to the inverter outpput during the interval

$$T_0 = T - T_1 - T_2$$

in each cycle.

As shown in Fig.2, in the transfering fron one to the other state, the switching sequence between the three voltage vectors involves only one commutation.

This obviously requires the use of both zero vectors (V_7 and V_8) in a given sector and a reversal of the switching sequence every cycle. The benefit of this switching sequence in Fig.3 is the reduction of commutation from four to three comparing to a regular sequence in Fig. 2.

The space vector modulation with the inversed sequence and the cycle frequency $f_c = \frac{1}{T}$ has the same number of inverter switching as the SPWM(Sinusoidal Pulse Width Modulation) with the carrier frequency, $f_{PWM} = \frac{f_c}{2}$.

III. The RMS values of the current ripple

From Fig.2, it is clear that the ripple waveform will be a periodic function with a period 2T. Neglecting the stator resistance and assuming the switching cycle T is essentially small with from t_3 and t_6 are calculated by :

$$i_\alpha(t_4) = i_{\alpha 0} + \left(\frac{E}{2} - \frac{2m}{4}\right)\frac{mTE}{2L\sigma} \quad (5)$$

$$i_\beta(t_4) = I_{\beta 0} + \left(\frac{\sqrt{3}}{2}\right)\frac{mTE}{2L\sigma}\left(1 - \frac{m}{2}\right) \quad (6)$$

$$i_{\alpha\beta}(t_5) = i_{\alpha\beta}(t_2) \quad (7)$$

$$i_{\alpha\beta}(t_0) = i_{\alpha\beta}(t_3) = i_{\alpha\beta}(t_6) = [I_{\alpha 0}, I_{\beta 0}] \quad (8)$$

where, $i_\alpha(t_0) = I_{\alpha 0}$, $i_\beta(t_0) = I_{\beta 0}$: initial values,

L_σ : The motor equivalent leakage inductance,

m : modulation index,

E : DC-bus voltage,

T : cycle period

The average value of α and β current components in the interval [$t_0 \cdots t_6$] of the proposed sequence in Fig.3 are given by :

$$i_\alpha^{av}(t_0, t_6) = \frac{mTE}{2L\sigma} \cdot \frac{3}{4}(1-m) + I_{\alpha 0}$$

$$i_\beta^{av}(t_0, t_6) = \frac{\sqrt{3}}{4} \frac{mTE}{2L\sigma}(1-m) \quad (9)$$

The RMS values of the α and β ripple components are given by :

$$\Delta i_{arms}^2 = \frac{1}{2T} \int_{t_0}^{t_6} i_\alpha^2(t)dt - (i_\alpha^{av})^2 \quad (10)$$

$$\Delta i_{\beta s}^2 = \frac{1}{2T} \int_{t_0}^{t_6} i_\beta^2(t)dt - (i_\beta^{av})^2 \quad (11)$$

The total ripple RMS value is given by

$$\Delta i_{\alpha\beta s}^2 = [\frac{mTE}{2L\sigma}]^2 [\frac{1}{4} - \frac{5m}{12} + \frac{m^2}{4}] \quad (12)$$

IV. Microprocessor based implementation

The determinations of intervals T_n, T_{n+1} and T_0 a re difficult for the microprocessor-based implemen tation. since the microprocessor requires powerful arithmetic capabilities and large memory space to store pulsewidth for a wide range of output volta ge and frequency. Therefore, to save the CPU ti me and look-up table memory and to avoid flo ating point operation, this paper propose the new algorithm that calculate the intervals of switchi ng vectors in Fig 3

The minimum number of pulse per half-cycle, P, which to calculate the pulse widths in the propos ed techniiique, is determined by:

$$P = \frac{f_c}{2f_r} = 9 + 6(K-1) \quad (13)$$

where, K=1,2 · · · ,n : integer,

f_c : the frequency of a triangular wave,

f_c : the frequency of a sine wave.

The modulation index, M is defined as :

$$M = \frac{A_r}{A_c} \quad (14)$$

where, A_c = the peak of carrier wave,

A_r = the peak of sine wave.

if f_c is much smaller than f_r as shown in Fig.5. the reference wave between the two intersectiosn points D and E can be picew-ise linear. Therefor e, the pulsewidths given by the space vector mod ulation method, ΔT , and the proposed method, ΔT. are approximately equal .

$$\Delta T' \cong \Delta T \quad (15)$$

From the similarity between △AFO and △ABK in Fig. 5, the following relation can be achieved :

$$\frac{1}{2}\Delta T : \frac{1}{2}T = (A_c - A_i) : A_c \quad (16)$$

where A_i = The amplitude of i-th sine wave at the center point of i-th triangular wave i = 1,2,3 · · · , [P/2+1]

[·]=Gauss operator.

From (16), i-th pulsewidth, ΔT_i , is given by :

$$\Delta T_i = T(1 - \frac{A_r}{A_c}) \quad (17)$$

From (14) and (16), the simple analytic form of e quation (17) is obtained:

$$\Delta T_i = T(1 - \frac{A_r}{A_c} M) \quad (18)$$

As shown in Fig. 6. the time intervals, ΔT_i ,bet ween the i-th and (i+1)-th pulsewidth is given b y:

$$\Delta T_{ti} = T(1 + \frac{A_i + A_{i+1}}{2A_r} M) \quad (19)$$

where, T_i =1,2, · · · I-1

During the positive-half cycle of reference sine w

ave, the driving transistor gating s-ignals are ge nerated by following operation :

TR On during the time interval of ΔT_i

TR Off during the time interval of ΔT_{ti}

During the negative-half cycle of reference sine wave, oppositegating gating signals of the positiv e-half cycle are generated.

The schematic diagram of an z-80 microprocessor -based voltage controlled inverter is shown in Fi g4.

V. Analytical and experimental results

Analytical results for the RMS value of the mot or current ripple are shown in Fig. 7. If both reg ular and optimized strategies have the same switc hing cycle, T, as shown in Figs.2-3, the optimize d strategies approach will have 25% fewer comm utation but will have an increasingly larger ripple than the regylar strategy for m >0.28, as the ripp le for reducing the number of commutation. Trace C in Fig 7 corresponds to the optimized sequence with a reduce cyc-le time T'=0.75T, having the s ame commutation frequency as the regular sequen ce, trace A, but will have an incresingly larger ri pple than the regular strategy for m>0.75

Trace D in Fig 7 with a re duce cycle time, T' = 0.5t has 25% fewer commutation frequency tha n trace A but will have lower ripple than the reg ular sequence over the full voltage range. The traces in Fig 7 suggest that the best result is o btained by the optimized strategy with a redu ced cycle time, T'=0.5T by reducing the cycle ti me T the motor current ripple is reduce as show n in Figs8-10, but switching losses are increased with the number of commutation.

Experimental result of the motor phase current an d the line voltage spectra are shown in Figs 8-1 3. The phase current waveform for m=0.8 is sho wn in Figs 9-10. At the rated speed, it can be seen that the optimized sequence results in a sign ificant-ly lower current ripple by reducing the c ycle time, T. The line voltage spectra of the wav eforms in Figs 8-10 are given in Figs 11-13. I n Fig 11. the line voltage spectrum has a predo minant components at the synchronous frequency of 57Hz and a relatively small component at 63H z, This small component is due to the relatively l arge harmonic distortion and current ripple. In Fi gs 12-13, predominant components are located at about 50hz, and relatively small components at ab out 70Hz. Thus, these large bandwidths between the main components and relatively small compon ents are due to small harmonic distortion and cur rent ripple. However, by reducing the cycle time, T, the synchronous frequency is lower than the r ated frequency of 60Hz because of increasing the slip.

Therefore, for maintaining V/f = constant, the mo tor current should be controlled by adjusting the DC generator.

VI. Conclusion

Characteristics of regular and proposed PWM se quence strategies are investigated both analyticall y and experimentally. The best analytical results are obtained by the proposed strategy with a red uced cycle time, T'=0.5T and confirmed by the e xperimental results of the motor phase current an d its line voltage spectra.

Since the proposed switching sequence is defined by simple analytic expressions such as equa 18-1 9, and required the minim-un number of pulse pe r half-cycle for the calculation of the pulsewidth, the proposed switching strategy is particularly s uitable for a minimal size memory microprocessor implementation.

For the modulation index, m, is less than 0.8 the proposed modulation strategy offers superior perfo rmance for majority of loads such as induction m otor drives.

Reference

[1] GRANT, T.L., and BARTON, T.H. "Control st rategie for PWM drivers", IEEE Trans, IA-16, pp 211-215, 1980

[2] A,J,Pollman, "Software Pulsewidth Modulation for microprocessor Control of AC Drivers". IEEE Trans, Ind, Appl, Vol IA-22 No. 4, pp691-696, jul

y/Aug. 1986
[3] J, Holtz, P. lammert, and W. Lotzkat: "High S peed Drive System with Ultrasonic MOSFET PW M Inverter and Single-Chip microprocessor Contr ol ", IEEE Trans . Ind Appl, Vol IA-23, No 6 pp 1010 - 1015 Nov/Dec. 1987
[4] H.W Van der Broeck, H.C. Skudelny, G,V S tanke :"Analyses and Realization of a Pulsewidth Modulator based on Boltage space Vectors ", IEE E Trans,Ind,Appl, IA-24, No.1, pp 142-150,jan/Fe b. 1988

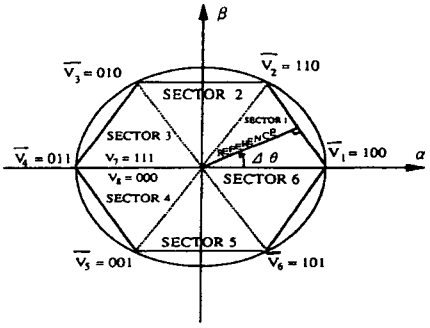

Fig. 1. Location of the inverter vectors $\overline{V_1}, \cdots \overline{V_8}$ in the $\alpha-\beta$ stationary frame.

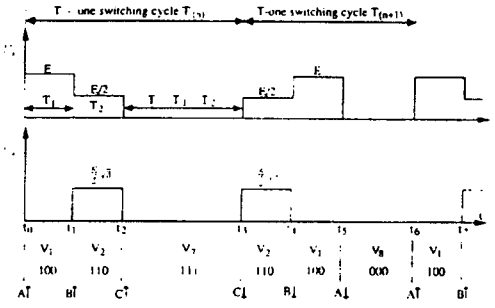

Fig. 2. Timing diagram for space vector modulation with proposed switching sequence and a reference vector in sector 1.

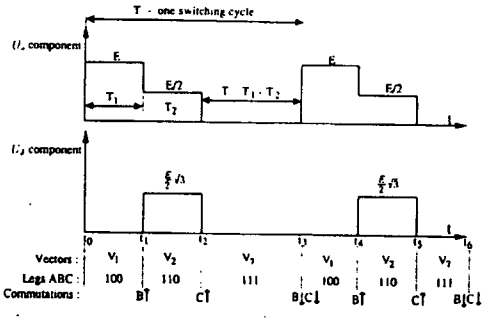

Fig. 3. Timing diagram for space vector modulation with regular switching sequence and a reference vector in sector 1.

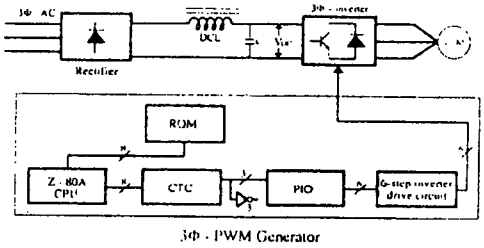

Fig. 4. The block diagram of an Z-80A microprocessor-based 3Φ-PWM Inverter.

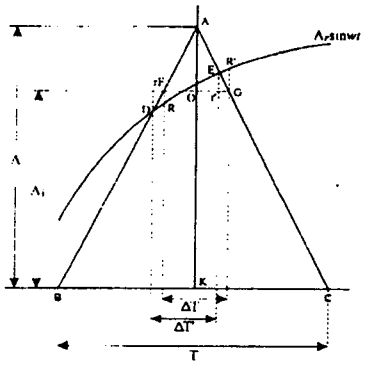

Fig. 5. Proposed PWM wavw generation strategy for micoroprocessor-based implementation.

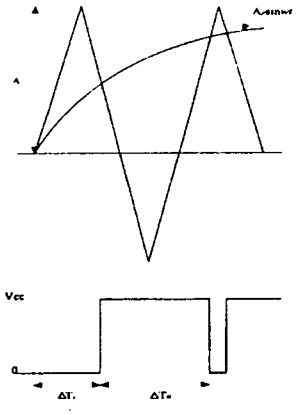

Fig. 6. The grting signals ΔT_i and ΔT_{ti} during the positive-half cycle of reference sine wave.

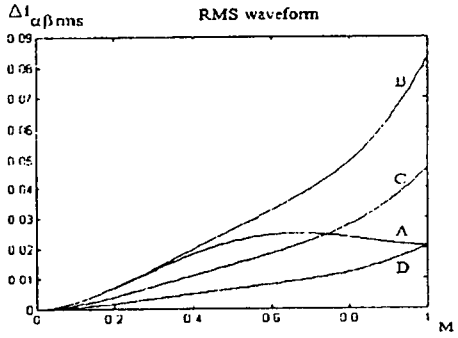

Fig. 7. the RMS value of the current ripple as a funtion of the modulation index, m. Trace A: with regular sequence, trace B: with optimized sequence, trace C: optimized sequence with reduced cycle time, T'=0.75T; trace D: with cycle time, T'=0.5T.

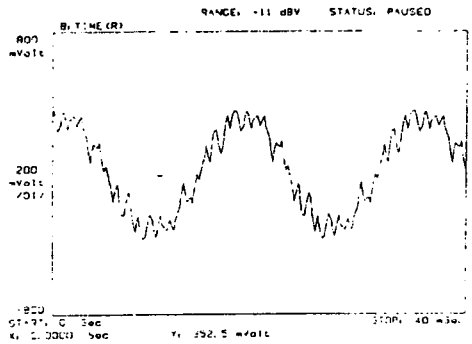

Fig. 8. Motor phace current, m=0.8, p=9, proposed sequence.

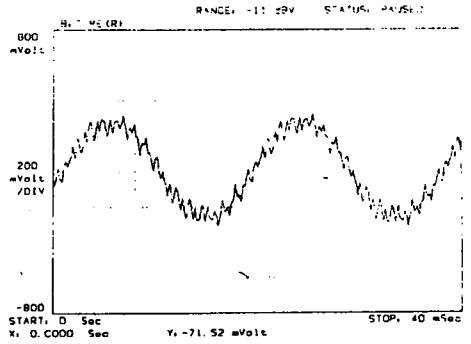

Fig.9. Motor phace current, m=0.8, p=15, proposed sequence.

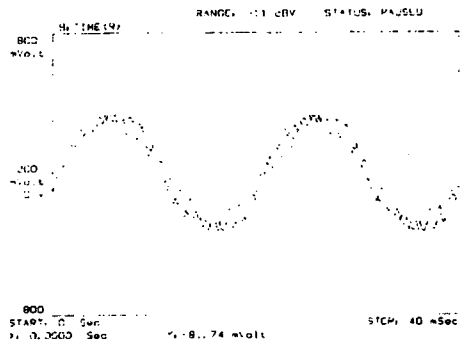

Fig. 10. Motor phace current, m=0.8, p=21, proposed sequence.

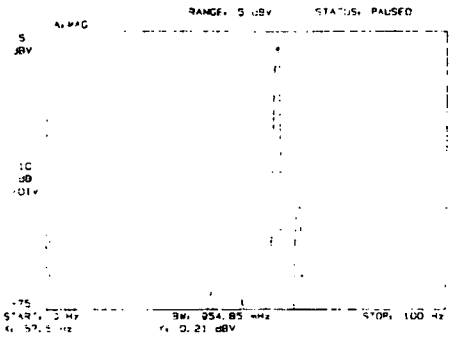

Fig. 11. Spectrum of the line voltage shown in Fig.8.

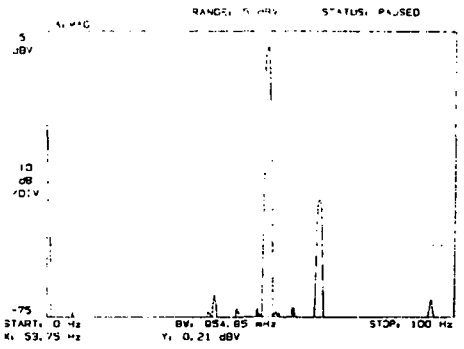

Fig. 12. Spectrum of the line voltage shown in Fig.9.

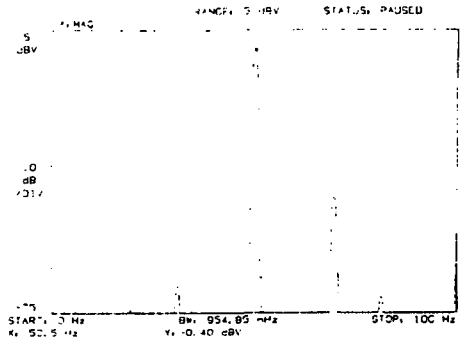

Fig. 13. Spectrum of the line voltage shown in Fig.10.

Table 1. Difinition of the voltage vectors avaible at inverter output, their α and β components and the inverter switching states.

VECTOR	ANGLE	U_α	U_β	STATES (●) 1 = HIGH ON 0 = LOW ON A	B	C	$\lvert \vec{U}_{out} \rvert$
$\vec{V}_1$	0°	E	0	1	0	0	E
$\vec{V}_2$	60°	$\frac{E}{2}$	$\frac{E}{2}\sqrt{3}$	1	1	0	E
$\vec{V}_3$	120°	$-\frac{E}{2}$	$\frac{E}{2}\sqrt{3}$	0	1	0	E
$\vec{V}_4$	180°	-E	0	0	1	1	E
$\vec{V}_5$	240°	$-\frac{E}{2}$	$-\frac{E}{2}\sqrt{3}$	0	0	1	E
$\vec{V}_6$	300°	$\frac{E}{2}$	$-\frac{E}{2}\sqrt{3}$	1	0	1	E
$\vec{V}_7$	-	0	0	1	1	1	0
$\vec{V}_8$	-	0	0	0	0	0	0